

Analysis of the oxygen potential of $\text{Th}_{1-y}\text{U}_y\text{O}_{2+x}$

R.P.C. Schram *

Nuclear Research and Consulting Group (NRG), P.O. Box 25, 1755 ZG Petten, The Netherlands

Abstract

Oxygen potentials of UO_2 – ThO_2 solid solutions ($\text{Th}_{1-y}\text{U}_y\text{O}_{2+x}$) were retrieved from the literature and analyzed. For each datapoint the oxygen pressure p_{O_2} , the nonstoichiometry x , the temperature T and the uranium concentration y was specified. The data were analyzed using the valency control model and the thermochemical model of Lindemer and Besmann for UO_{2+x} which was extended for the analysis of the $\text{Th}_{1-y}\text{U}_y\text{O}_{2+x}$ data. The solid solution is regarded as an ideal ternary solution of UO_2 , ThO_2 and a hypothetical compound U_aO_b . The thermodynamic properties of this compound U_aO_b were determined in two oxygen pressure ranges of the database. In this thermochemical approach ThO_2 is treated as an inert solvent that does not participate in any of the chemical equilibria describing the oxygen potential.

© 2005 Elsevier B.V. All rights reserved.

1. Introduction

Nuclear energy is generated in reactors which use uranium as fuel, in almost all cases in the form of the oxide UO_2 . The major part of the nuclear reactors world-wide are light–water reactors, in which uranium is slightly enriched in the fissile isotope ^{235}U . A disadvantage of this type of fuel is that it produces long-lived transuranium elements through neutron capture in ^{238}U . These elements contribute significantly to the long-term radiotoxicity of the high-level waste. The use of thorium-based nuclear fuels may substantially reduce the amount of actinides produced in the nuclear fuel cycle. With this type of fuel the fissile ^{233}U is formed by neutron capture without formation of transuranium elements. However, since thorium (^{232}Th) is not fissile, thorium-containing fuel must contain some startup material such as uranium (^{235}U) or plutonium (^{239}Pu).

Therefore, mixtures of ThO_2 and UO_2 are considered as good candidates for thorium-fuelled reactors.

For the fabrication of the fuel and for the understanding of its behaviour under normal and off-normal conditions, it is important to know the chemical characteristics of $\text{Th}_{1-y}\text{U}_y\text{O}_{2+x}$. One of the important quantities in the thermochemistry of $\text{Th}_{1-y}\text{U}_y\text{O}_{2+x}$ is its chemical potential of oxygen, or oxygen potential, which plays a decisive role in the interaction of the fuel with the cladding (corrosion) and the formation of fission product compounds. The oxygen potential depends on the uranium content y , the amount of excess oxygen x and the temperature T . In the present assessment, only hyperstoichiometric oxides are considered; oxygen potential measurements of hypostoichiometric ($x < 0$) $\text{Th}_{1-y}\text{U}_y\text{O}_{2+x}$ were not found in the literature. Data of both hypostoichiometric uranium oxide [1] and hypostoichiometric thorium oxide [2] are available in the literature, however. In Section 2 a description of the data retrieval is given.

In Section 3 the models for the oxygen potential of $\text{Th}_{1-y}\text{U}_y\text{O}_{2+x}$ are derived. First the valency control

* Tel.: +31 224 564 362; fax: +31 224 568 608.
E-mail address: schram@nrg-nl.com

model is investigated. In this model it is assumed that the oxygen potential is determined by the valency of uranium. The scaling behavior of the oxygen potentials versus the mean uranium valency is investigated in Section 3.1.

In Section 3.2 a more empirical approach is presented. Lindemer and Besmann applied a thermochemical model to the oxygen potentials of UO_{2+x} [1] and $\text{Pu}_{1-y}\text{U}_y\text{O}_{2+x}$ [3] and CeO_{2-x} [4]. It was shown that $\text{Pu}_{1-y}\text{U}_y\text{O}_{2+x}$ could be described as a quaternary mixture of UO_2 , PuO_2 , and the hypothetical oxides $\text{Pu}_{4/3}\text{O}_2$ and either $\text{U}_2\text{O}_{4.5}$ or U_3O_7 [3]. More recently, the Lindemer and Besmann model was applied to AmO_{2-x} [5]. Similarly, we will assume that $\text{Th}_{1-y}\text{U}_y\text{O}_{2+x}$ can be described as a mixture of UO_2 , ThO_2 and the hypothetical compound U_aO_b . The stoichiometric coefficients a and b determine the slope of the oxygen potential when plotted versus $\ln x$. The stoichiometric coefficients and the enthalpy of formation of U_aO_b are obtained for two oxygen potential ranges by fitting the derived oxygen potential curve. The discussion of the results is given in Section 4.

2. Database

Oxygen potential data were either read from tables or taken from graphs. The graphs were digitized and then analyzed using a digitizing programme. The error that is introduced by the digitizing procedure, either resulting from low resolution of the original or from deformation of the graph copy, was not larger than 1 percent relative error. These errors were determined by measuring reference points on the coordinate axes of the graphs. A total of 339 x - y - T - p_{O_2} datapoints were retrieved from the literature (Table 1).

Some of the oxygen potential data are presented as a function of the uranium valency V_{U} . For example, the data of Anderson et al. [6] were read from a graph of the oxygen pressure versus the mean uranium valency for different values of y and T . The amount of excess oxygen x was calculated using the relation for the mean

uranium valency: $V_{\text{U}} = 4 + 2x/y$ (see Section 3.1). The measurements of Roberts et al. [7] were tabulated as the oxygen pressure versus the uranium concentration y . The excess amount of oxygen was calculated from the given uranium concentration y and a fixed uranium valency of 4.35 [7].

The retrieved oxygen potentials are related to the oxygen pressures using:

$$\Delta \bar{G}_{\text{O}_2} = RT \ln(p_{\text{O}_2}/p_{\text{O}_2}^{\circ}), \quad (1)$$

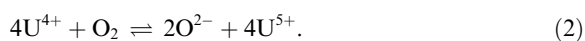
where p_{O_2} is the oxygen pressure in MPa and $p_{\text{O}_2}^{\circ}$ is the standard-state pressure (0.1 MPa). Plots of the oxygen potential versus the coordinates x , y and T are shown in Fig. 1.

3. Oxygen potential models for $\text{Th}_{1-y}\text{U}_y\text{O}_{2+x}$

3.1. Valency control model

A simple scaling model for the oxygen potential of nonstoichiometric solids is the valency control model in which it is assumed that the oxygen potential is fully determined by the mean valency of uranium V_{U} [10,13]. As was pointed out by Ugajin [10] the oxygen potentials of UO_{2+x} and $\text{Th}_{1-y}\text{U}_y\text{O}_{2+x}$ are equal at a given uranium valence only if the $(\text{U,Th})\text{O}_2$ solution is ideal. Close to stoichiometry the uranium valence seems to be a good scaling parameter for $\text{Th}_{1-y}\text{U}_y\text{O}_{2+x}$ [10]. For $\text{Pu}_{1-y}\text{U}_y\text{O}_{2+x}$ a similar observation was made for the hypostoichiometric oxide [15].

In this model, that was earlier applied to UO_{2+x} [13], it is assumed that uranium has either the +4 or the +5 valency state:



The reaction Gibbs energy is:

$$\Delta_r G = -RT \ln \frac{[\text{O}^{2-}]^2 [\text{U}^{5+}]^4}{(p_{\text{O}_2}/p_{\text{O}_2}^{\circ}) [\text{U}^{4+}]^4}. \quad (3)$$

Table 1
Oxygen potential measurements of $\text{Th}_{1-y}\text{U}_y\text{O}_{2+x}$

Authors	Year	y -Range	Method ^a	T (K)	# Datapoints
Anderson et al. [6]	1954	0.03–0.244	TGA/V	1003–1203	33
Roberts et al. [7]	1958	0.0053–0.0597	PM	1123	6
Aronson and Clayton [8]	1960	0.29–1	EMF	1250	47
Tanaka et al. [9]	1972	0.048–0.295	EMF	1250	16
Ugajin et al. [10–12]	1982	0.05–1	TGA	1273–1473	58
Matsui and Naito [13]	1985	0.2–1	TGA	1282–1373	155
Anthonyamy et al. [14]	1997	0.54–0.9	EMF	1073–1173	24

^a EMF = electromotive force measurements; TGA = thermogravimetric analysis; V = gas volumetric method; PM = pressure measurement.

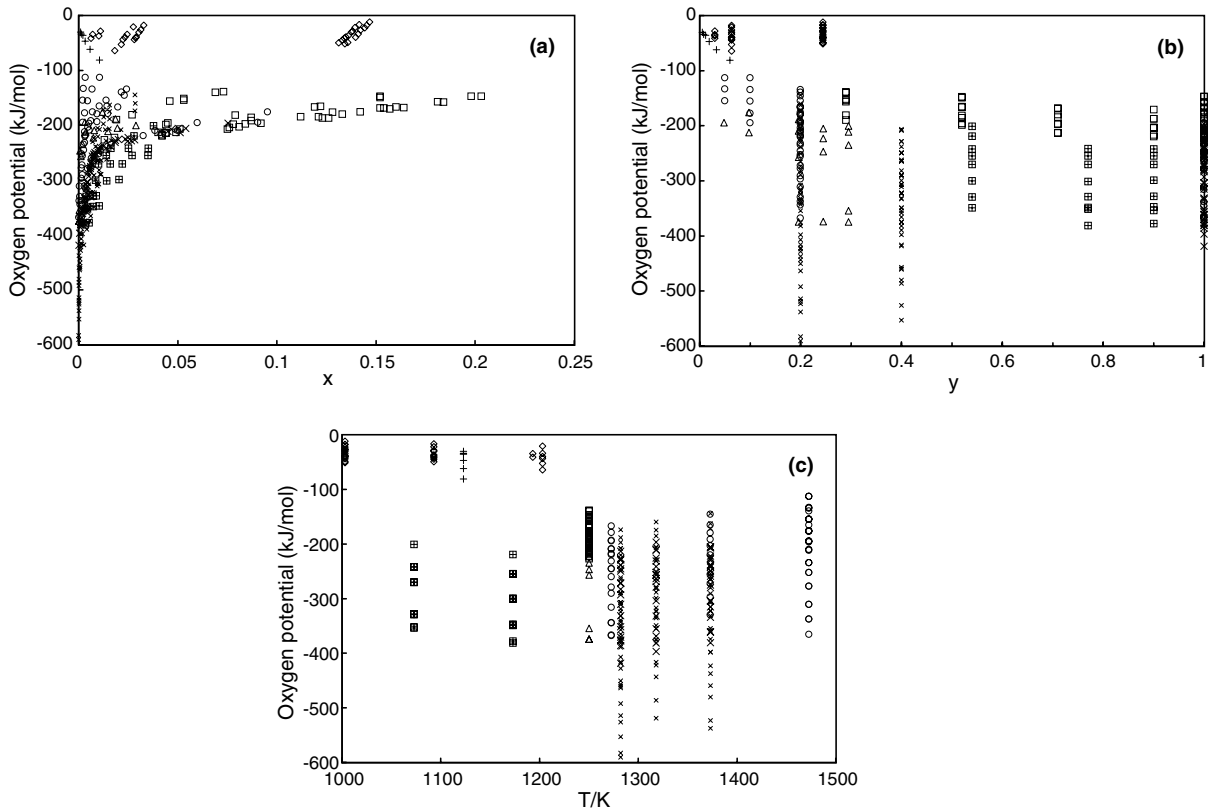


Fig. 1. The oxygen potential database of Th_{1-y}U_yO_{2+x}: (a) oxygen potential versus x (b) oxygen potential versus y (c) oxygen potential versus T . Oxygen potentials higher than -100 kJ mol^{-1} : (\diamond): Anderson et al. [6]; (+): Roberts et al. [7] Oxygen potentials lower than -100 kJ mol^{-1} : (\square): Aronson and Clayton [8]; (\triangle): Tanaka et al. [9]; (\circ): Ugajin et al. [10–12]; (\times): Matsui and Naito for $y = 1$ [13]; (small \times): Matsui and Naito for $y = 0.2, 0.4$ [13]; (\boxplus): Anthonyamy et al. [14].

After applying the mass balance for uranium and oxygen and the electroneutrality equation, it can be shown that the oxygen potential is a function of the uranium valency [13]:

$$\Delta \bar{G}_{\text{O}_2} = 2RTf(V_{\text{U}}) + \Delta_r H^\circ - T\Delta_r S^\circ, \quad (4)$$

with

$$f(V_{\text{U}}) = 2 \ln \frac{V_{\text{U}} - 4}{5 - V_{\text{U}}} + \ln \left(\frac{V_{\text{U}}}{2} \right). \quad (5)$$

Eq. (4) describes the oxygen potential as a function of V_{U} and T . It can be shown that the mean uranium valence is $V_{\text{U}} = 4 + 2x/y$ for the mixture Th_{1-y}U_yO_{2+x}.

All oxygen potential data of Th_{1-y}U_yO_{2+x} smaller than -100 kJ mol^{-1} were fitted to this equation, which resulted in $\Delta_r H^\circ = -522676.50 \text{ J mol}^{-1}$ and $\Delta_r S^\circ = -298.96 \text{ JK}^{-1} \text{ mol}^{-1}$. The temperature range of the database is $T = 1003 \text{ K}$ to $T = 1473 \text{ K}$ and the mean temperature is approximately $T = 1250 \text{ K}$. In order to compare the measurements at different temperatures the following scaling function is used [1]:

$$\begin{aligned} \ln(p_{\text{O}_2}/p_{\text{O}_2}^\circ)(T = 1250 \text{ K}) \\ = \ln(p_{\text{O}_2}/p_{\text{O}_2}^\circ)(T) + \frac{\Delta_r H^\circ}{R} \left\{ \frac{1}{1250} - \frac{1}{T} \right\}. \end{aligned} \quad (6)$$

The results are shown in Fig. 2. For the highest oxygen potentials, i.e. the lowest uranium concentrations, the experimental datapoints deviate from the scaling curve. For lower oxygen potentials the scaling function works well, except for the data of Matsui and Naito [13] for $y = 0.2$ and 0.4 , and the measurements of Anthonyamy et al. [14]. This will be discussed in Section 4.

For the present database, it is found that the scaling of the oxygen potential with the uranium valence is reasonably good for oxygen potentials smaller than -100 kJ mol^{-1} and uranium valences up to 4.6.

3.2. Thermochemical description

A different way of describing the oxygen potential of nonstoichiometric oxides is the thermodynamical model of Lindemer and Besmann [1]. It supposes that UO_{2+x}

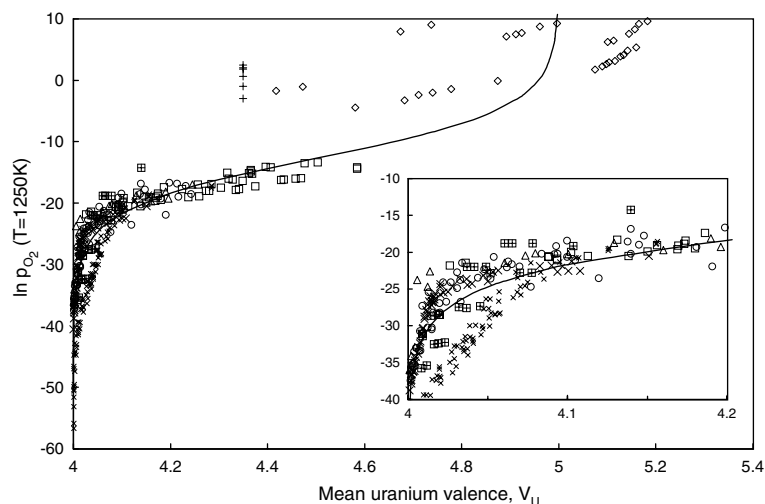
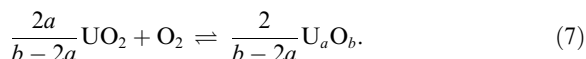


Fig. 2. The scaled oxygen potential of $\text{Th}_{1-y}\text{U}_y\text{O}_{2+x}$ versus V_U . Symbols as in Fig. 1. Solid line: Eq. (4) scaled to 1250 K using Eq. (6).

can be regarded as a mixture of stoichiometric UO_2 and a hypothetical compound U_aO_b . The O/M ($=2+x$) ratio specifies the amount of U_aO_b present in the mixture. The oxygen potential can be evaluated from the equilibrium between both uranium oxides:



It can be shown that the oxygen potential is given by:

$$\begin{aligned} \Delta\bar{G}_{\text{O}_2} &= RT \ln(p_{\text{O}_2}/p_{\text{O}_2}^\circ) \\ &= \frac{2}{b-2a} RT \ln \frac{[\text{U}_a\text{O}_b]}{[\text{UO}_2]^a} + \Delta_r H^\circ - T \Delta_r S^\circ, \end{aligned} \quad (8)$$

where $\Delta_r H^\circ$ and $\Delta_r S^\circ$ are the enthalpy and entropy of the reaction described in Eq. (7). The brackets denote the chemical activity of the compound, and we assume that it equals the mole fraction of this compound (ideal model). We will assume that ThO_2 cannot take up excess oxygen and therefore does not appear in the chemical equilibrium. In this assumption, ThO_2 is chemically inert, but it does of course appear in the mass balance of $\text{Th}_{1-y}\text{U}_y\text{O}_{2+x}$. The activities $[\text{U}_a\text{O}_b]$, and $[\text{UO}_2]$ can be calculated from the mass balances of U, Th, and O. It can be shown that the oxygen potential is a function of the oxygen excess x and the uranium concentration y :

$$\Delta\bar{G}_{\text{O}_2} = 2RTf(x, y) + \Delta_r H^\circ - T \Delta_r S^\circ, \quad (9)$$

with

$$f(x, y) = \frac{1}{b-2a} \ln \frac{x\{b-2a+(1-a)x\}^{a-1}}{\{(b-2a)y-ax\}^a}. \quad (10)$$

In order to compare the measurements at different temperatures Eq. (6) is applied which results in:

$$\begin{aligned} \ln(p_{\text{O}_2}/p_{\text{O}_2}^\circ)(T = 1250 \text{ K}) \\ = 2f(x, y) + \frac{\Delta_r H^\circ}{1250R} - \frac{\Delta_r S^\circ}{R}. \end{aligned} \quad (11)$$

Eq. (11) is the fit equation that will be used to fit the experimental values of x , y , T and $(p_{\text{O}_2}/p_{\text{O}_2}^\circ)$ with the fit parameters a and b , $\Delta_r H^\circ$ and $\Delta_r S^\circ$.

Fitting all oxygen potentials with a single set of parameters (a , b , $\Delta_r H^\circ$ and $\Delta_r S^\circ$) did not give satisfactory results. Better fit results were obtained by fitting the oxygen potentials larger and smaller than -100 kJ mol^{-1} separately. For the oxygen potential data smaller than -100 kJ mol^{-1} , a total of 180 datapoints, including 94 datapoints for $y = 1$, were considered in this fit. The data of Matsui and Naito [13] for $y = 0.2$ and 0.4 and the data of Anthonysamy [14] were not used in the fitting procedure (see Discussion).

The data of Roberts et al. [7] and Anderson et al. [6] refer to small values of y and slightly lower temperatures. These oxygen potentials are larger than -100 kJ mol^{-1} and were fitted separately. For this fit, 39 datapoints were considered.

The fit parameters are given in Table 2 and the results are shown in Fig. 3.

A plot of the fit for oxygen potential data smaller than -100 kJ mol^{-1} is given in Fig. 4. This shows the x - and y -dependence of the oxygen potential at a fixed

Table 2
Fit parameters of Eq. (11)

Oxygen potential range	$\Delta_r H^\circ$ (J mol^{-1})	$\Delta_r S^\circ$ ($\text{J K}^{-1} \text{ mol}^{-1}$)	a	b
$< -100 \text{ kJ mol}^{-1}$	-426929	-226.95	1.289	3.232
$> -100 \text{ kJ mol}^{-1}$	-114230	-23.02	1.974	5.21

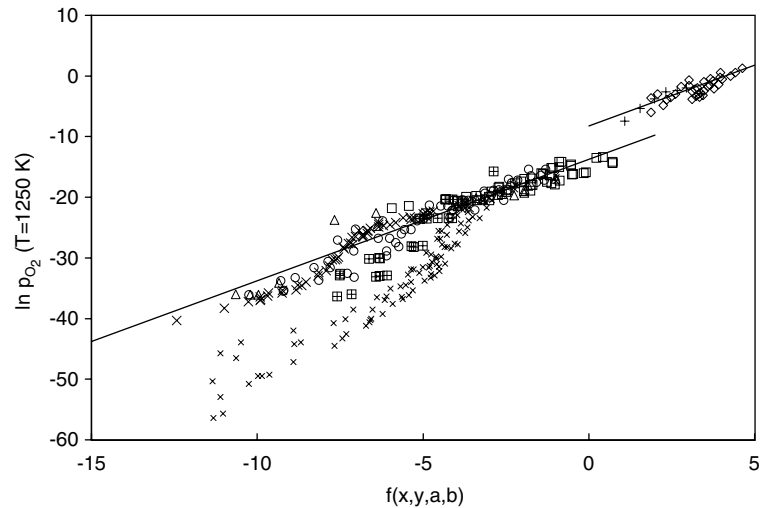


Fig. 3. Results of the fit using the thermochemical model. Symbols as in Fig. 1. Solid lines: Eq. (11). Fit parameters, see Table 2.

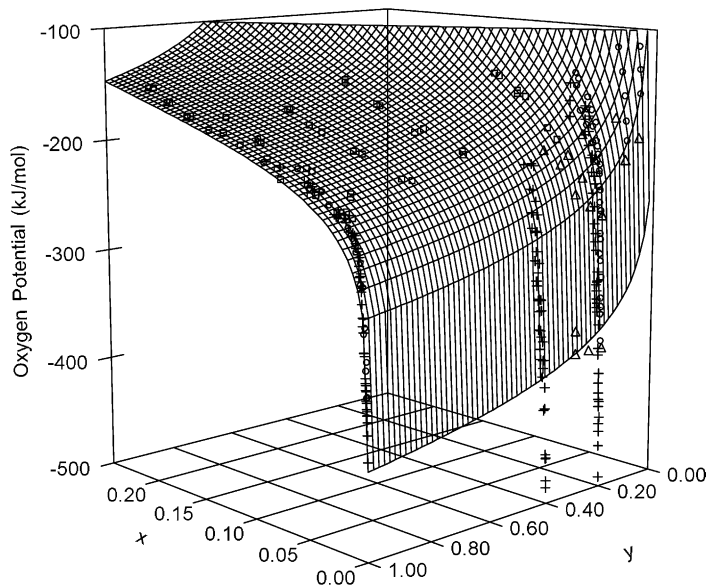


Fig. 4. Oxygen potential versus x and y according to the thermochemical model. The experimental datapoints ($T = 1003$ K to $T = 1473$ K) are specified in Table 1. The solid surface is calculated using Eq. (11) with the fit parameters for the range < -100 kJ mol⁻¹ at $T = 1250$ K.

temperature of $T = 1250$ K. For small values of y the oxygen potential becomes very high.

4. Discussion

The results of the thermochemical model are shown in Fig. 5. All the 339 experimental datapoints (including the rejected datapoints) are shown in this plot. Excluding the rejected data, the accuracy of the thermo-

chemical model is $\pm 20\%$ (or ± 50 kJ mol⁻¹) for oxygen potentials < -100 kJ mol⁻¹ and $\pm 45\%$ (or ± 20 kJ mol⁻¹) for oxygen potentials > -100 kJ mol⁻¹. Pronounced differences between the oxygen potential of Th_{1-y}U_yO_{2+x} were found in the work of different authors. For all measurements considered, the oxygen potential increases with increasing temperature, increasing x and decreasing uranium concentration y (this behaviour is also predicted by the two models investigated in this paper). The only exception are the data of Matsui and Naito

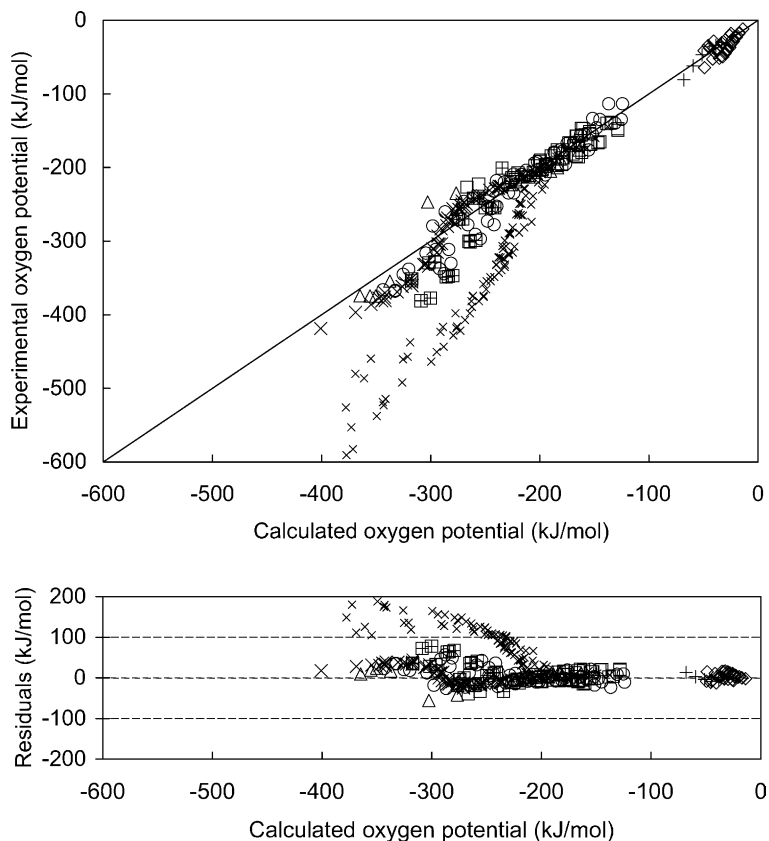


Fig. 5. Result of the thermochemical description. Symbols as in Fig. 1. The data below and above -100 kJ mol^{-1} are calculated using different sets of fit parameters.

[13] for $y = 0.2$ and 0.4 . These data were not used in the fitting procedure of the thermochemical model because of the fact that these $\text{Th}_{1-y}\text{U}_y\text{O}_{2+x}$ oxygen potentials are smaller than experimentally determined values of UO_{2+x} for the same values of x and T , which is not in agreement with the other $\text{Th}_{1-y}\text{U}_y\text{O}_{2+x}$ data sets and which is also not in agreement with the predictions of both models presented in this paper. In addition, the data of Anthonysamy et al. were not used. The scaling behaviour of these data points versus the uranium valency (see Fig. 2) is different from the other measurements and good fitting results within the thermochemical model could not be obtained.

The origin of the differences between the various oxygen potentials measurements is not quite clear. The found differences may be related to the experimental error in the nonstoichiometry x which is discussed in reference [16]. The nonstoichiometry is obtained experimentally by measuring the weight increase of the sample after each change in the oxygen potential. Therefore, an error in the initial stoichiometric oxygen potential (at $x = 0$) can result in an offset in the complete x -range. The errors in the excess oxygen concentrations x are

estimated to be ± 0.001 [10] or even ± 0.01 [8]. Another source of errors may be the oxygen potential at stoichiometry. The oxygen potential of the stoichiometric mixed oxide $\text{Th}_{1-y}\text{U}_y\text{O}_2$ is set by exposing a pellet of this substance to a gas mixture with a specified oxygen potential. This is a crucial step, for any change in the oxygen potential close to stoichiometry has a significant effect on the value of x . The oxygen potentials used to obtain the stoichiometric oxide range from $-589.1 \text{ kJ mol}^{-1}$ [13] to -376 kJ mol^{-1} [10]. It is therefore very important to know what the oxygen potential of the stoichiometric oxide is and if equilibrium is attained. More series of oxygen potential measurements, with special attention for the reference oxygen potential of the stoichiometric mixed oxide $\text{Th}_{1-y}\text{U}_y\text{O}_2$, would be required to solve these inconsistencies.

Within the valency control model it was assumed that uranium has either the +4 or the +5 valency state, which implies that V_U cannot exceed 5. Earlier attempts to fit the +4/+6 valency state model did not give satisfactory results [13]. An interesting aspect of the thermochemical model is that the uranium valency is not fixed. In fact the valency of uranium is either +4 (in UO_2) or $2b/a$ (in

U_aO_b). When the obtained fit parameters are inserted, we find that the valency of uranium in U_aO_b is 5.02 (for $<-100 \text{ kJ mol}^{-1}$) or 5.29 (for $>-100 \text{ kJ mol}^{-1}$). These results suggest that the uranium valency is indeed either +4 or +5.

Both the valency control model and the thermochemical model rely on the assumption that ThO_2 can be considered as an inert solvent that does not take part in the chemical equilibria that describe the oxygen potential. This is justified by the measurements of Aitken et al. [17], who measured the activity of uranium oxide in $\text{Th}_{1-y}\text{U}_y\text{O}_{2+x}$ using the transpiration method and found that the stoichiometric UO_2 – ThO_2 solution is ideal at $T = 1573 \text{ K}$. In this context it is interesting to note that UO_2 and ThO_2 mix in all proportions, and that the cubic (fluorite-type) solutions follow Vegard's law closely [18]. In agreement herewith both models describe the thorium concentration dependence of the oxygen potential quite well.

5. Conclusion

A database of oxygen potential data of $\text{Th}_{1-y}\text{U}_y\text{O}_{2+x}$ was constructed and analyzed. Both the experimental data and the model-predictions show that the oxygen potential of $\text{Th}_{1-y}\text{U}_y\text{O}_{2+x}$ increases with (i) increasing temperature, (ii) increasing oxygen excess x , and with (iii) decreasing uranium concentration y .

The valency control model was applied to the $\text{Th}_{1-y}\text{U}_y\text{O}_{2+x}$ and shows that the mean uranium valency is a good scaling parameter for oxygen potentials below $<-100 \text{ kJ mol}^{-1}$ and V_U smaller than ≈ 4.6 .

The empirical approach of Lindemer and Besmann was applied successfully to $\text{Th}_{1-y}\text{U}_y\text{O}_{2+x}$. This thermo-

chemical model assumes that $\text{Th}_{1-y}\text{U}_y\text{O}_{2+x}$ can be described as an ideal mixture of UO_2 , ThO_2 and a hypothetical compound U_aO_b . Using this approach analytical expressions for the oxygen potentials were derived that describe the oxygen potentials smaller than -100 kJ mol^{-1} and oxygen potentials larger than -100 kJ mol^{-1} separately.

References

- [1] T. Lindemer, T. Besmann, *J. Nucl. Mater.* 130 (1985) 473.
- [2] R. Ackermann, M. Tetenbaum, in: *Thermodynamics of Nuclear Materials*, vol. 1, 1980, p. 29.
- [3] T. Besmann, T. Lindemer, *J. Nucl. Mater.* 130 (1985) 489.
- [4] T. Lindemer, T. Besmann, *Calphad* 10 (1986) 129.
- [5] C. Thiriet, R. Konings, *J. Nucl. Mater.* 320 (2003) 292.
- [6] J. Anderson, D. Edgington, L. Roberts, E. Wait, *J. Chem. Soc.* (1954) 3324.
- [7] L. Roberts, L. Russel, A. Adwick, A. Walter, M. Rand, in: *Proc. Intern. Conf. Peaceful Uses Energy*, 2nd., Geneva, vol. 28, 1958, p. 215.
- [8] S. Aronson, J. Clayton, *J. Chem. Phys.* 32 (3) (1960) 749.
- [9] H. Tanaka, E. Kimura, A. Yamaguchi, J. Moriyama, *J. Jpn. Inst. Metals* 36 (7) (1972) 633.
- [10] M. Ugajin, *J. Nucl. Mater.* 110 (1982) 140.
- [11] M. Ugajin, T. Shiratori, K. Shiba, *J. Nucl. Mater.* 116 (1983) 172.
- [12] M. Ugajin, *J. Nucl. Sci. Technol.* 20 (3) (1983) 228.
- [13] T. Matsui, K. Naito, *J. Nucl. Mater.* 132 (1985) 212.
- [14] S. Anthonysamy, K. Nagarajan, P.V. Rao, *J. Nucl. Mater.* 247 (1997) 273.
- [15] R. Woodley, *J. Nucl. Mater.* 96 (1981) 5.
- [16] K. Park, D. Olander, *High. Temp. Sci.* 29 (1990) 203.
- [17] E. Aitken, J. Edwards, R. Joseph, *J. Phys. Chem.* 70 (4) (1966) 1085.
- [18] K. Bakker, E. Cordfunke, R. Konings, R. Schram, *J. Nucl. Mater.* 250 (1997) 1.